BOREAL ENVIRONMENT RESEARCH 20: 227–242
ISSN 1239-6095 (print) ISSN 1797-2469 (online)

Helsinki 30 April 2015

Atmospheric CO_2 observations at Finnish urban and rural sites

Juho Kilkki[1)], Tuula Aalto[1)], Juha Hatakka[1)], Harri Portin[2)] and Tuomas Laurila[1)]

[1)] *Finnish Meteorological Institute, P.O. Box 503, FI-00101 Helsinki, Finland*
[2)] *Finnish Meteorological Institute, P.O. Box 1627, FI-70211 Kuopio, Finland*

Received 2 Dec. 2013, final version received 7 May 2014, accepted 8 May 2014

Kilkki J., Aalto T., Hatakka J., Portin H. & Laurila T. 2015: Atmospheric CO_2 observations at Finnish urban and rural sites. *Boreal Env. Res.* 20: 227–242.

Four new ground-based atmospheric monitoring stations in Finland were examined for local and large-scale signals in carbon dioxide mole fraction, and the results were compared with the corresponding values obtained from WMO/GAW site Pallas, northern Finland and NOAA/ESRL marine boundary layer reference time series. The measurements were filtered with knowledge of local weather and air composition. Periods of a presumably well-mixed boundary layer and relatively pollutant-free air were close to the Pallas time series in mole fraction, particularly in the winter. Wintertime mole fractions were 5–10 ppm higher than the signal in the marine boundary layer at all stations. The seasonal amplitude was 18–24 ppm, and diurnal amplitude was 0–3 ppm in winter and 3–20 ppm in the summer months. All stations, with the possible exception of the urban site in Helsinki, showed potential for observing a large-scale carbon dioxide signal.

Introduction

Due to the role it plays in the carbon cycle and long-term influence on climate, carbon dioxide (CO_2) molar fractions have been tracked globally for decades — most notably at the Mauna Loa observatory, Hawaii, where the yearly mixing ratio of CO_2 constantly increased from 315 ppm between the beginning of continuous measurements in 1958 to 396 ppm in 2013 (Keeling *et al*. 1976, Ballantyne *et al*. 2012; for current data *see* NOAA/ESRL Trends in Carbon Dioxide, http://www.esrl.noaa.gov/gmd/ccgg/trends/). Molar fractions have also been measured in the marine boundary layer, providing information on background spatial and temporal variations; and at locations less representative of global background, but providing essential information on variations above continents (NOAA/ESRL Cooperative Air Sampling Network, http://www.esrl.noaa.gov/gmd/ccgg/; WMO Global Atmosphere Watch World Data Centre for Greenhouse Gases, http://ds.data.jma.go.jp/gmd/wdcgg/).

Tropospheric molar fractions carry information about carbon fluxes over vast areas. The bottom-up approach to quantify the CO_2 exchange — inventories of anthropogenic emissions and biomass and soil carbon changes, and use of in situ measurements, remote sensing data and process modeling — is subject to uncertainties. Upscaling these results to a regional or continental scale is sensitive to the choice of measurement location, heterogeneity of land use and its representation, and integrity of emission estimates (Beer *et al*. 2010, Luyssaert *et al*. 2007, Jung *et al*. 2011). An application of a continental trace gas measurement network is the evaluation of surface fluxes by combining direct mole fraction

Editor in charge of this article: Veli-Matti Kerminen

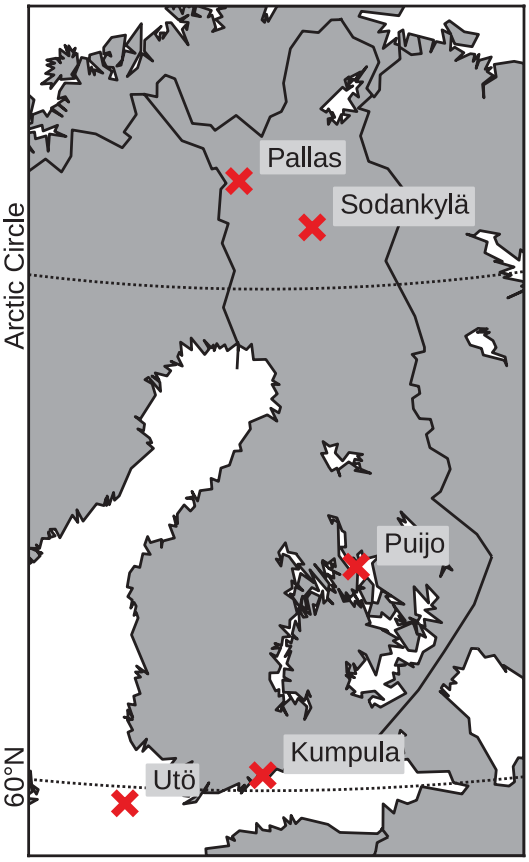

Fig. 1. Map of Finland and locations of measurement sites.

measurements with atmospheric transport models (e.g. Rödenbeck *et al*. 2003). By increasing the amount of continental measurement stations, the CO_2 balance can be assessed using this top-down approach, providing an independent measure of the net source strength. At present, a reasonable flux accuracy can be obtained at a scale of 1000 km in western Europe, where the density of continental measurement stations is highest (Carouge *et al*. 2010). The purpose of this study is to examine the benefit of extending the use of observations to less suitable locations, such as those near strong local, anthropogenic CO_2 sources.

We examined the local and regional impacts on measurements carried out at four low-altitude stations in Finland, both in urban and rural settings (Kumpula, Helsinki; Puijo, Kuopio; and Sodankylä Geophysical Observatory) and in a marine location (Utö). Atmospheric CO_2 observations from these new stations are reported here for the first time. We compared the results with the National Oceanic and Atmospheric Administration (NOAA) marine boundary layer (MBL) reference (Conway *et al*. 1994, Masarie and Tans 1995; http://www.esrl.noaa.gov/gmd/ccgg/mbl/), and data obtained from World Meteorological Organization (WMO) Global Atmosphere Watch (GAW) station Pallas, an arctic hill site at the northern border of the boreal zone. A clean background signal can be extracted from a noisy data record with local influences by using appropriate filtering routines (Thoning *et al*. 1989, Padin *et al*. 2007), and in this study, information on meteorological conditions and air composition was used. Effectiveness of the filters was examined and their appropriate use at different stations evaluated. The time series were obtained using optical spectrometers, which are calibrated to meet the network accuracy requirements for use in global inversions (Masarie *et al*. 2011, Rödenbeck *et al*. 2006).

Material and methods

Sites

The five sites analyzed are in the northern part of Europe, locations extending from hemi-boreal to subarctic climate zones: urban site (Kumpula in Helsinki), marine site in the northern Baltic Sea (Utö), semi-urban site (Puijo), and two sites in the northern boreal zone (Sodankylä and Pallas) (Fig. 1 and Table 1).

We compared measurements with the NOAA/ESRL MBL dataset representing large air masses, obtained from coastal and marine sites around the world (for documentation and relevant stations *see* http://www.esrl.noaa.gov/gmd/ccgg/mbl/). The data were represented as a smoothed function of time and latitude. For each marine site, a function consisting of a variable amount of polynomial and harmonic terms was fitted to the entire time series in order to obtain a smoothed dataset by applying a low-pass filter to the residual. These series were fitted to obtain the latitudinal distribution progression over time, which could be used to construct a zonal reference time series for a given latitude, comparable to the time series utilized in this study.

Pallas

The Pallas node of the Pallas–Sodankylä station is a GAW monitoring network station of the WMO. Continuous CO_2 measurements began in 1996. The CO_2 record of the Pallas site was extensively examined by Aalto *et al*. (2002) and Eneroth *et al*. (2005), and it was found to provide an accurate measurement of large-scale CO_2 features when selected for air mass history.

The Pallas measurement site in Pallas–Yllästunturi National Park is located on the top of an arctic hill (Sammaltunturi, 565 m a.s.l.) (Hatakka *et al*. 2003). It is located at the southern edge of a 50-km-long chain of arctic hills, the highest peak of which reaching 809 m a.s.l. Air is sampled above the roof of the building at 7 m above ground, but the hilltop rises 100 m above the tree line and 257 m above the nearby lake (Pallasjärvi). Local and regional anthropogenic CO_2 sources are weak. The biggest towns in the region are Muonio (2500 inhabitants, 19 km to the west) and Kittilä (6000 inhabitants, 46 km to the southeast). There is a gold mine 55 km to the east. Vegetation on the rocky hilltop is sparse and low, mostly consisting of mosses and lichens. Surrounding ecosystems include boreal forests, wetlands and lakes, typical tree species being Scots pine (*Pinus sylvestris*), Norway spruce (*Picea abies*) and downy birch (*Betula pubescens*).

Sodankylä

In Sodankylä, CO_2 measurements were conducted at the Finnish Meteorological Institute (FMI) Arctic Research Center, which is the other node of the Pallas–Sodankylä GAW station. It is located 5 km to the south from the town of Sodankylä (8800 inhabitants). Some office and research buildings are found within 1 km. A river runs in the northwest–southeast direction at a distance of 300 m on the west side of the mast. Further away there is a low-traffic road. The station is surrounded by coniferous forests and wetlands of a fen type. The distance to the extensive mire to the east is 0.5 km. The most common tree species is Scots pine, and the forest floor is covered by moss, lichen and shrubs. The average annual temperature is around –1 °C, and on a typical year, the ground is permanently covered by snow from October to May. The average height of the Scots pine forest canopy is 12 m, and air was sampled at 48 m above ground from a mast.

Puijo

Puijo is an observation and telecommunications tower in the city of Kuopio. Meteorological measurements, and air quality and aerosol measurements began in 2005 and 2006, respectively,

Table 1. Location of the measurement sites, and description of climate and ecosystem type.

	Utö	Kumpula	Puijo	Sodankylä	Pallas
Coordinates	59°47.034´N, 21°22.030´E	60°12.228´N, 24°57.654´E	62°54.564´N, 27°39.309´E	67°21.708´N, 26°38.290´E	67°58.400´N, 24°06.939´E
Elevation a.s.l. (m)	8	24	231	179	565
Measurement level (m above ground)					
CO_2	57	30	80/85*	48	7
Wind	50	32	80	22	7
Station type	mast	building	tower	mast	hill
Ecosystem	barren archip.	urban	urban, boreal	boreal	tundra
Typical vegetation	shrubs	mixed forest	conifers	conifers, peatland	shrubs
Permanent snow cover	Jan–Mar	Dec–Apr	Nov–Apr	Sep–May	Oct–May
Mean temperature (°C)					
Warmest month (since 2010)	16.8 (Jul 2012)	22.2 (Jul 2010)	18.6 (Jul 2011)	14.2 (Jun 2013)	13.1 (Jul 2011)
Coldest month (since 2010)	–3.1 (Mar 2013)	–10.8 (Jan 2010)	–12.0 (Feb 2012)	–15.8 (Feb 2012)	–15.2 (Feb 2011)

* the measurement height was raised by 5 m on 5 October 2011.

at the highest level of the tower (Leskinen *et al*. 2009). The FMI and the University of Eastern Finland together maintain the measurements. Greenhouse gas measurements started as Demo Experiment of the European Integrated Carbon Observing System (ICOS). The 75-m tall Puijo tower is on a hill that rises 150 m above the surrounding lakes. The air sampling height was 5 m above the roof of the tower, at 80 m above ground (raised to 85 m in 2011). The Kuopio town center is 2–3 km southeast from the measurement station, and residential areas are found to the north, east and south. A highway runs from north to south on the east side, passing by at a 1 km distance. Total local population is 105 000 (as of 2013), and besides the city itself, other possible local CO_2 sources include a waste landfill (10 km southwest), a power plant (3 km south), and a paper mill (5 km northeast). The station is surrounded by boreal forests, lakes and smaller patches of agricultural land. The most common tree species are Scots pine and Norway spruce.

Kumpula

The measurements in Kumpula (Helsinki) were carried out from the roof of the FMI building located on a hill. The main roads and traffic emissions are about 45 m below the sampling level. Downtown Helsinki is 4 km to the south, and the Baltic Sea at a distance of 1 km. Helsinki is located on the southern coast of Finland. The metropolitan area extends 20–30 km from the city center and is populated by just over a million people. The site can be described as semi-urban. It is surrounded by residential and commercial buildings, roads, parks, forests, and gardens. The road to the east is a major source of CO_2 emissions during rush hours. The most common tree species around the site are birch (*Betula* sp.), Norway maple (*Acer platanoides*), aspen (*Populus tremula*), goat willow (*Salix caprea*) and bird cherry (*Prunus padus*). Air was sampled 6 m above the roof, 30 m above ground.

Utö

Utö is an island on the outskirts of the Archipelago Sea in the Baltic Sea about 80 km southwest from the mainland Finland. Open sea is in the wind sector 80°–300°. The island is about 1 km^2 in size, mostly rocky and treeless. Typical vegetation is low and consists of grass and shrubs. Mean annual temperature is 6.5 °C. Permanent ice cover is present on average from mid-February to early April, and in the winter of 2012–2013, the sea was also frozen during March. In the winter of 2013–2014, there was no permanent ice cover. The annual net flux over the Baltic Sea is quite small; the Baltic Proper is a carbon sink between April and September, and otherwise a source (for details *see* Wesslander 2011). The population of the island is in the dozens. Local emissions include mainly small boats and a ferry to the mainland, which might stay overnight in the harbor. The harbor is used by small boats exclusively, but large cruise and cargo ships frequently pass 6–40 km to the south, and some cargo ships 1.5 km to the west, of the island. Measurements were carried from a cell phone mast at 57 m above ground and 65 a.s.l., about 200 m from the coast.

Measurements

The measurements are based on cavity ring-down spectroscopy (CRDS) instruments from Picarro Inc. (Santa Clara, CA). The long, optical path length of the instrument allows for measurements with high precision, using near-infrared laser sources (Crosson 2008). The resulting spectrograms are analyzed and converted into mixing ratios by the instrument. Winds were measured by Adolf Thies UA2D sonic anemometers at all sites, with the exception of Utö, where a Metek USA-1 by Metek GmbH (Germany) was used.

Instruments took their sample air with their own vacuum pumps, i.e. there were no sample pumps upstream of the instrument inlet. Sample flow through the instrument was ca. 200 ml min^{-1} depending on the instrument type and sample pressure. All the stations, except for Kumpula, had an absolute pressure controller (MKS 640 with all metal seals) before the Nafion® drier, or before the instrument inlet if there was no dryer. Where there was one,

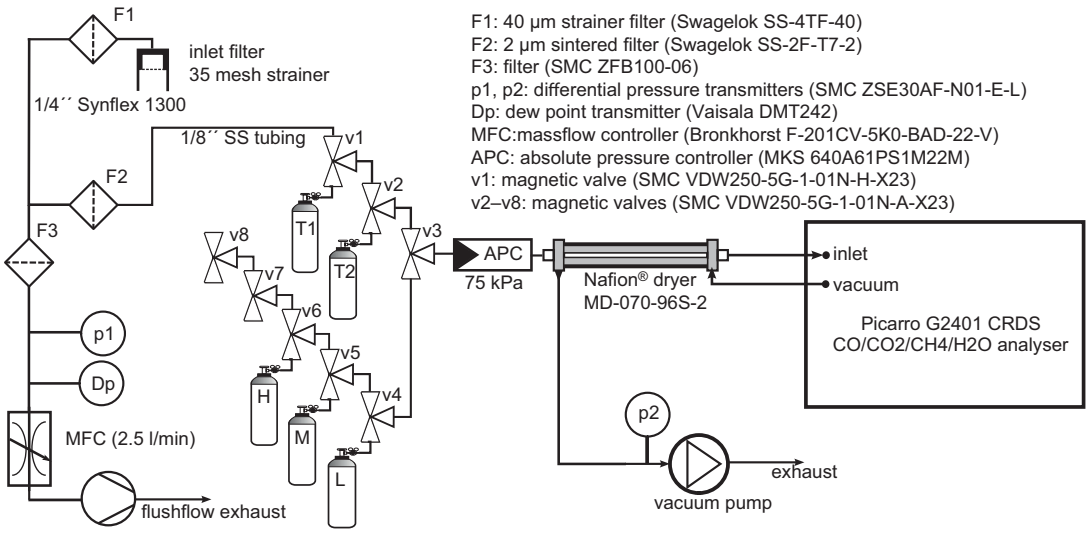

Fig. 2. Flow diagram of the CO_2 measurement system at Utö.

reference and so-called target gases were also ran through the dryer. This controller kept the sample pressure, and thus flow rate, constant for all the incoming gas streams. The measured gas stream was selected with magnetic valves controlled by a custom-made program running on instrument's computer. The magnetic valves used were SMC Pneumatics VDW250-5G-1-01N-A-X23 (brass, oil-free specification) for dry gases and VDW250-5G-1-01N-H-X23 for the sample (stainless steel, oil-free specification). The filter at the gas-stream select-valve inlet was the Swagelok Inline Filter with 2 μm nominal pore size sintered element (SS-2F-2). In addition, there were inlet filters at Puijo and Utö: Swagelok Tee-Type Filter with 40 μm nominal pore size strainer element (SS-4TF-40). To prevent inlet freezing at Pallas, Puijo, and Utö, a heating cable was wrapped around the inlet. The sampling line heating was implemented by installing a heating cable (ca. 5 W m^{-1}) together with the sampling line (two lines at Utö and Puijo) inside an outer tube, which was wrapped tightly around the heating cable and sampling lines (i.e. no insulation). At Sodankylä, the horizontal lines were insulated. The flow diagram of the Utö measurement system is depicted in Fig. 2. Other stations had similar systems, with some differences due to drying/no drying, inlet, and how the flushing was arranged.

All the data from the CRDS instruments, together with auxiliary measurements (e.g. flow rate, sample and vacuum line pressures, room temperature), were stored as one-minute averages, and these averages were used in further data processing. This included making a water vapor correction (i.e. getting dry mixing ratio), taking into account calibrations made for the instrument, and flagging out erroneous results due to e.g. maintenance and technical problems.

We measured both Nafion®-dried sample air with a residual water vapor mixing ratio of about 0.1%–0.2%, and wet (not dried) sample air. Rella *et al*. (2013) showed that the WMO/GAW targets can be achieved using the water vapor mixing ratio measured by the analyzer and correct by it to get the dry air mole fractions. Details of the CO_2 instruments at different sites as well as sample air drying method are given in Table 2, whereas sample inlet, line and residence times are presented in Table 3.

Each site had either one or two target gas cylinders, one of which was measured at least two times a day (Table 4). Results for these gases were calculated as for the ambient sample air, and they were used as an indication of the instrument's performance (e.g. noise and drift). Two sites (Pallas, Kumpula) used WMO/GAW Central Calibration Laboratory (CCL, i.e. NOAA/ESRL/GMD) calibration gases, which

were measured manually a few times a year. The Puijo ICOS Demo site used a set of three standard gases, and initially also two target gases, made and calibrated by the Max-Planck-Institute for Biogeochemistry, Jena. The other two sites used station standard gases made by FMI. These

Table 2. Instruments used for CO_2 measurements. Nafion® dryer was Perma Pure MD-070-96S-2.

Site	Measurement period	Instruments (Picarro)	Sample drying
Pallas	Jan 2010–Nov 2011	G1301	Nafion®
	Nov 2011–	G2401	Nafion®
Sodankylä	Nov 2011–May 2012	G2301	Nafion
	Jun 2012–	G2401	Nafion®
Puijo	Jul 2011–May 2012	G2301-m	Nafion®
	Jun 2012–	G2301-m	No drying
Kumpula	May 2010–Jan 2011	G1301	Nafion®
	Jan 2011–	G1301	No drying
Utö	Mar 2012–	G2401	Nafion®

Table 3. Instrumentation: inlet types and filters, sample lines, total flow rates and sample residence times from inlet to instrument.

Site	Inlet	Sample line/manifold	Flow rate	Sample residence time (s)
Pallas	56 mm inner diam. SS-tube both up and down, heated	15 m, 56 mm inner diam. (60 mm outer diam.) acid resistant stainless steel (SS) tubing	130 m^3 h^{-1}	1
Sodankylä	6 mm inner diam. SS-tube downwards	73 m, 6 mm inner diam. (8 mm outer diam.) SS tubing	2.2 l min^{-1}	56
Puijo	17 mm brass tube 40 μm filter downwards, heated	22 m, 4.3 mm inner diam. (1/4´´ outer diam.) Synflex 1300 tubing	2.2 l min^{-1}	10
Kumpula	56 mm inner diam. SS-tube upwards	15 m, 51 mm inner diam. (57.6 mm outer diam.) PVC tubing	25 m^3 h^{-1}	5
Utö	17 mm brass tube 40 μm filter downwards, heated	124 m, 4.3 mm inner diam. (1/4´´ outer diam.) Synflex 1300 tubing	2.7 l min^{-1}	40

Table 4. Target and calibration gas measurements for the CRDS systems.

Site	Target gas how often/duration	Calibration gases	Calibration how often/duration (per cylinder)
Pallas	T1: 7 h/15 min T2: 21 h/15 min	7 WMO/CCL standard gas cylinders	4–6 times a year/20–50 min
Sodankylä	T1: 11 h/15 min T2: 28 h/20 min	3 station standard gas cylinders (FMI)	every 11 days/40 min
Puijo	T1: 9 h/12 min T2: 37 h/15 min	3 ICOS Demo standard gas cylinder	every 12 days/15 min
Kumpula	T: 7.5 h/15 min	2 WMO/CCL standard gas cylinders	2–3 times a year/30 min
Utö	T1: 9.5 h/15 min T2: 28.5 h /18 min	3 station standard gas cylinders (FMI)	every 8 days/34 min

gases had been calibrated by the FMI at least two times against WMO/CCL standard gases. Automatic calibration was made at these three latter sites (Puijo, Utö and Sodankylä). Average target gas mixing ratio differences from the assigned values were within –0.04 to +0.01 ppm, with a standard deviation between 0.02–0.07 ppm. Minimum and maximum differences were within –0.2 to +0.2 ppm.

For Pallas, Sodankylä and Kumpula, an approximately linear calibration drift was recorded. One-minute-average raw wet values were first corrected with the water vapor correction factors determined experimentally for each instrument to get the dry uncalibrated mixing ratios. These mixing ratios were plotted against time since the first calibration for each calibration gas cylinder. For some instruments, this produced a linear time dependent (and mixing ratio independent) function, which was used to reduce the one-minute dry values back to the time of the first calibration. Calibration was determined based on these values, and for all the instruments this produced a constant (not time dependent) linear calibration equation. This method was applied when calculating mixing ratios for the target cylinders and sample air.

For two stations with a relatively high station standard sampling frequency, Utö and Puijo, the calibration coefficients were smoothed with a two-month wide Blackman–Harris rolling window to calibrate the outdoor measurements as well as samples from the target cylinders. The coefficients were derived from linear calibration determined for several days a month (Table 4) by sampling air from three station standard cylinders. To correct for water vapor effects, default correction factors were used, introducing an error of up to 0.15 ppm compared with instrument-specific factors.

Pallas

The CRDS instrument took its sample air from the main manifold via a 3-m-long, 2.1-mm-inner diameter and 1/8´´-outer diameter stainless steel tubing. A Nafion® dryer was installed before the instrument inlet port, and it was run with dried air as purge air until November 2011, after which it was run in reflux mode. This change caused no noticeable change in the target cylinder measurement results. A pressure controller was installed before the Nafion® dryer in June 2012.

Sodankylä

The mast had inlets at four heights: 2, 10, 23 and 48 m. From the lines at 2, 23 and 48 m, a sample for the CRDS system was taken with a 6-m, 2.1-mm inner diam. (1/8´´ outer diam.) stainless steel tubing. The sample air from 2 and 23 m was buffered in 10 liter volumes and measured once an hour for 5 minutes each. The line from the 48-m height was not buffered, and it was measured the rest of the time, excluding target and station standard cylinder measurements. Although the inlet was not heated, the horizontal sample lines were insulated and heated during winter to prevent them from freezing closed. A Nafion® dryer was installed before the instrument's inlet port, and it was run in reflux mode. A pressure controller was installed before the Nafion® dryer on January 2012.

Puijo

Puijo was an ICOS Demo site, and there were two CRDS instruments running in parallel, one measuring non-dried sample and the other sample air dried with Nafion® until 31 May 2012. After that, only the non-dried measurements were continued with an instrument that was earlier measuring dried sample air. The sampling tube was 22-m long (4.3 mm inner diam.; 1/4´´ outer diam.). A pressure controller was installed before the CRDS instrument in June 2012. For filtering out locally polluted air, mole fractions of nitrogen oxides (NO_x) measured with a TEI42i manufactured by Thermo Electron Corp. (Mass., USA) were used.

Kumpula

Sample air was taken from the roof of the FMI's building as a side flow of a main flow going to the radon (Rn) measurement system. The

CRDS system took its sample air via a 4-m-long, 4.3-mm-inner-diam. (1/4´´ outer diam.) stainless steel tubing. Equilibrium equivalent radon abundance was measured with a system, in which air is drawn alternately through two filters in 4-h periods. Beta activity on filters was continuously recorded with Geiger-Müller counters. The radon mole fraction was calculated from the measured flow rate, beta-efficiency of the counters, and count rate increase assuming that the increase was due to short-lived radon progeny only (Paatero *et al*. 1994). Covariation of CO_2 with nitrogen oxides and carbon monoxide (CO) was examined to flag polluted air samples. Gas concentrations were measured at a height of 4 m by TEI42S (NO_x) Thermo Electron Corp. (Mass., USA) and APMA370 (CO) by Horiba Ltd. (Japan).

Utö

Sample air was taken from an inlet on a cell phone mast at the 57-m height through a 124-m, 4.3-mm-inner-diam. (1/4´´ outer diam.) tube. There was also a sensor measuring temperature and relative humidity, and a 3D sonic anemometer installed at the same height. The line was heated during winter.

Results

Time series

Measurements have been continuous since 1996 in Pallas, and since 2010–2012 at the other four stations, from the height levels examined. In Kumpula, there was a gap in measurements in the winter of 2011–2012. The CO_2 mole fraction time series from all sites show a cycle of higher mole fractions in winter and lower mole fractions in summer (Fig. 3). In addition, different sites show higher frequency mole fraction variation in the scale of days. This variation is brought by air masses with diverse transport patterns, originated from changes in the weather systems that occur at the scale of several days to months. If air masses are transported over a distant region with considerable emissions, the trace of this signal is seen in the mole fraction record. Sometimes the signal was simultaneously visible at several sites. These variations were saved here, and not filtered away by e.g. tracing air mass history.

Diurnal variation

The unfiltered diurnal cycles at Sodankylä, Puijo and Kumpula exemplify continental CO_2 progression in the lower planetary boundary layer. In summer, photosynthesis draws the mole fraction down during the day: the mole fraction reaches its minimum in late afternoon (17:00–20:00), and peaks in the early hours of the morning. During the winter months, the only consistent feature of the diurnal progression is a rise in hourly mole fractions in Kumpula after 7:00–8:00. We attribute this spike to the morning rush hours. During the whole measurement period, apparent solar at all the sites time was within 40 minutes of the local winter time.

The amplitude of diurnal variation of CO_2 mole fraction ranged from 0–3 ppm in winter to 3–20 ppm in late summer (Fig. 4). In July and August, when environmental driving factors enable the largest biogenic sources and sinks, the amplitude of average diurnal cycle was at its maximum at all continental sites (11–20 ppm). The amplitudes were largest in Sodankylä and Kumpula, reflecting the low altitude and continental location of the sites. Wintertime persistence of systematic diurnal variation in Kumpula may have been caused by local anthropogenic sources, such as traffic. Diurnal boundary layer dynamics and consequent mixing of CO_2 into an air layer of varying height may also play a role. The filtering process described in the following section reduces the diurnal amplitudes by up to half, particularly during the summer months and at polluted sites (Kumpula and Puijo) in winter.

In Utö, the diurnal variation of CO_2 mole fraction in July–August was weaker than at Pallas. In addition to the absence of strong sources and sinks of CO_2 in the marine environment, the nocturnal temperature inversion was weak, inhibiting pronounced CO_2 anomalies near the surface. As compared with that at the continental sites, the diurnal cycle phase was lagged,

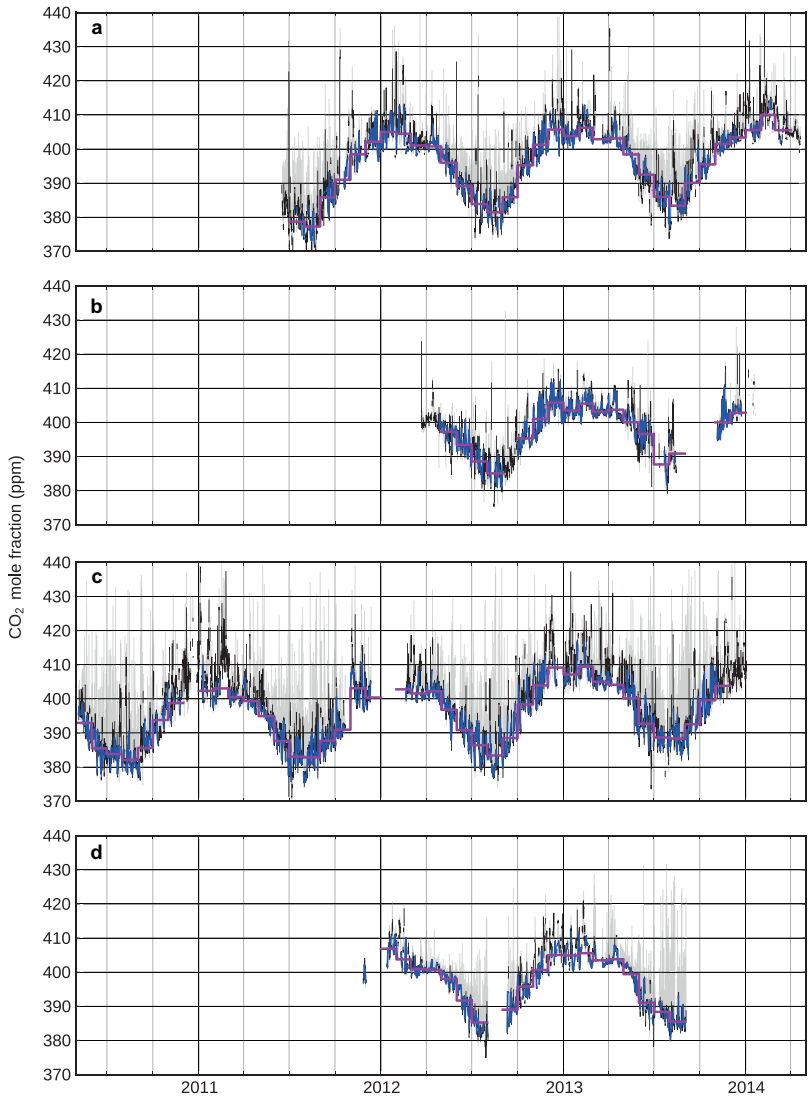

Fig. 3. Time series of CO_2 mole fraction at (**a**) Puijo, (**b**) Utö, (**c**) Kumpula, and (**d**) Sodankylä: hourly averages (grey lines), hourly values between 12:00 and 18:00 (black lines), daily time series after filtering, obtained from the afternoon hourly averages (blue lines); monthly averages of filtered daily values (magenta lines).

the average mole fraction being relatively constant during the day (8:00–16:00) and decreasing to a minimum in the early hours.

The Pallas measurement site is above the nocturnal boundary layer, which explains the lower summertime amplitude, as CO_2 released by plants is trapped by the inversion below the measurement point. As compared with Kumpula and Puijo, the high latitude and near-arctic conditions may play a role at Pallas as well. However, the measurements at a lower altitude in Sodankylä suggested a diurnal amplitude comparable to that at Pallas.

Filtering

To obtain data representing large-scale features, local influences like nearby traffic or ecosystem emissions have to be minimized. We filtered the measurements with meteorological parameters (wind speed and direction), composition of the sampled air (pollution) and hourly standard deviation of one-minute CO_2 mole fractions. When pollution or wind speed data were not available, no averages were calculated. Due to the low planetary-boundary-layer height, insufficient mixing and consequent poor representativeness of measurements, as well as difficulty in

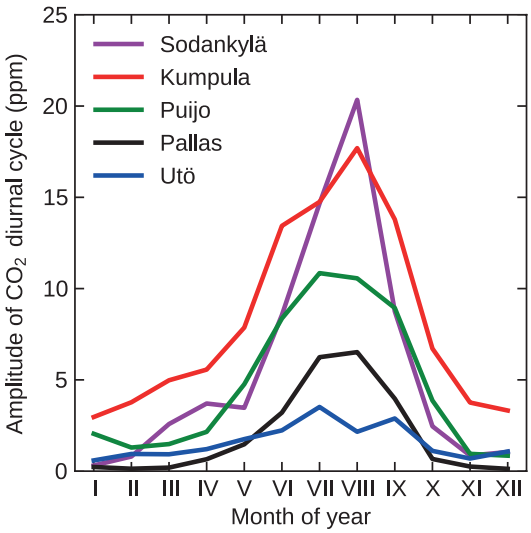

Fig. 4. Peak-to-peak CO_2 diurnal amplitudes for each station and month of the year. Amplitudes are determined from 4 sinusoid least-squares harmonic fits to detrended and deseasonalized unfiltered mole fractions for each month and station.

modeling nighttime fluxes, we considered only afternoon data (12:00–18:00 local time). Using afternoon means as daily averages is consistent with Haszpra (1999). As Utö is a marine site with a weak mean diurnal cycle of both CO_2 and temperature (and stability), only afternoon values were used in the averaging scheme for Utö as well. The afternoon selection was also implemented for the whole dataset from Sodankylä, although that site is north of the Arctic Circle and the cycle of shortwave radiation in midwinter is weak (the polar night lasts for several days in late December). This selection was implemented, in part, for a consistency with other sites.

The wind speed was averaged over 10-minute periods (except for Sodankylä, where the data were hourly), and each one-minute period was filtered from the averaging scheme if the wind speed was below a threshold value specified for each site individually. The averaging period of 10 minutes is of the order of the turbulent time scale of a convective boundary layer, and it was employed to smooth out most large eddies. The results were not sensitive to this averaging period. At Puijo, the wind sectors corresponding to individual point sources were filtered. Here 10-minute averages were used as well.

Typically, in the study region, the lower-tropospheric wind speed peaks in winter. Consistent with this, the median wind speed was at its minimum in June–July, at least in Utö and Puijo. However, considering only the afternoon averages that are associated with a better-mixed planetary boundary layer in summer than in other seasons, the difference to wintertime values was not clear and we employed a constant threshold wind speed for every station.

To select the cases with a low temporal variation, standard deviations of one-minute averages were determined for each hour, and periods exceeding a certain (arbitrary) value were left out. The underlying assumption here was that local-point sources leave a high-frequency trace signal in the time series. Owing to the seasonal cycles in planetary boundary layer dynamics and biogenic sinks and sources, the median hourly standard deviation varied highly with the season: in Utö, Puijo and Sodankylä, a clear peak in the standard deviation of CO_2 mole fraction was found in June–August, reaching about 0.4 ppm, and a minimum in late winter (March–April, 0.1 ppm). While being more aggressive in the summer than other times of the year, a constant standard deviation filter was implemented for each station.

The filters described above were aggressive in summer when the median wind speed tends to be low and its variation within an hour high. For Kumpula, however, wintertime values were most aggressively selected out by the filtering process, due to the seasonality in the median hourly standard deviation that was highest durinh the winter months (December–February). The contrast with other sites was possibly caused by local anthropogenic emissions (traffic in particular), trapped in the poorly-mixed wintertime planetary boundary layer. Despite the seasonality, constant thresholds were used in all filters. More elaborate filters can be applied in the future, when there will be more data so that we will get a more robust estimate of the seasonal changes and the effect of the filters on the data record.

To remove the remaining, exceptionally high (low) values, which usually indicate poorly-mixed air masses with a local source (sink) signature, filtered hourly and daily mean values

deviating too much from a long-term average were removed. The long-term increase in the CO_2 mole fraction and its seasonal cycle were represented by a function of polynomial and harmonic terms, respectively:

$$\sum_{i=1}^{p} a_i t^{i-1} + \sum_{j=1}^{h} b_j \sin\left(2\pi jt + \phi_j\right)$$

where, t is the time expressed in years, and a_i, b_j, and ϕ_j are constants determined by the means of a least-squares fit to the time series. Considering that only 1–3 years of data were available for each station, two polynomial (p = 2) and three harmonic terms (h = 3) were used in the fit. Three times the standard deviation of the residual was used as a limit.

For the Sodankylä time series, the wind speed data obtained from about 20 m above ground were used. At this level, the wind speed was distinctly attenuated during the winter months when the planetary boundary layer was stable. For this reason, a wind speed limit of 1.5 m s^{-1} and a relatively aggressive 0.6 ppm standard deviation limit were used. Results were consistent around all wind directions. In Puijo, the CO_2 mole fraction peaked in the wind sectors 30°–60° and 150°–180°. These sectors correspond to a local paper mill (5 km) and power plant (3 km), respectively. The data associated with these wind sectors were ignored in the averaging scheme. In Utö, in the direction of the mast (south west), the wind speed data were highly underestimated, effectively masking data from all air coming from that direction. This was also the prevailing wind direction, facing the open sea. We compared the time periods when the wind was blowing from either the continent or open sea at both Utö and Kumpula. No visually significant wind direction dependence was found for the mole fraction or diurnal cycle of CO_2 at either station. However, NO_x and CO, emitted by the traffic, depend on the wind direction at Kumpula (see also Aalto *et al*. 2009).

For the Puijo and Kumpula time series, we used air quality measurements to remove some of the influence of the city and nearby roads. The minute averages with the dry air mole fraction of NO_x above the threshold value of 5 ppb and 15 ppb in Puijo and Kumpula, respectively, were filtered (Table 5). In Kumpula, CO and radon data were also available but, due to gaps in the data and association of NO_x with anthropogenic sources, they were ignored as superfluous. Many discernible periods of a high CO_2 mole fraction were associated with high levels of NO_x.

Finally, monthly averages were calculated as the arithmetic means of the afternoon averages for periods with at least five days of available

Table 5. Range of the measurement period, CO_2 mole fraction filtering specifications, percentage of hourly averages passing filter (excluding afternoon selection), and amplitudes of diurnal and seasonal cycles, as determined from the unfiltered and filtered data sets, respectively.

	Utö	Kumpula	Puijo	Sodankylä	Pallas
Measured since	Mar 2012	May 2010	Jun 2011	Nov 2011	Oct 1996
Measured until	Mar 2014	Jan 2014	Mar 2014	Sep 2013	Jan 2010
Median wind speed (m s^{-1})	7.2	4.1	7.2	2.2	6.5
Median std dev. (ppm)	0.20	0.61	0.34	0.20	0.13
Wind speed below (m s^{-1})	2.5	3.0	3.0	1.8	4 (winter), 3 (summer)
hourly CO_2 std dev. below (ppm)	0.6	0.8	0.7	0.7	0.3 (winter), 0.5 (summer)
NO_x high limit (ppb)	–	20	4	–	–
Rn high limit (Bq m^{-3})	–	2	–	–	–
Excluded sectors	–	–	30–60° and 150–180°	–	–
Hourly values Passing filter (%)	69	61	56	59	69
July–Aug diurnal amplitude	3	17	11	18	6
Seasonal cycle amplitude	18	22	24	22	18

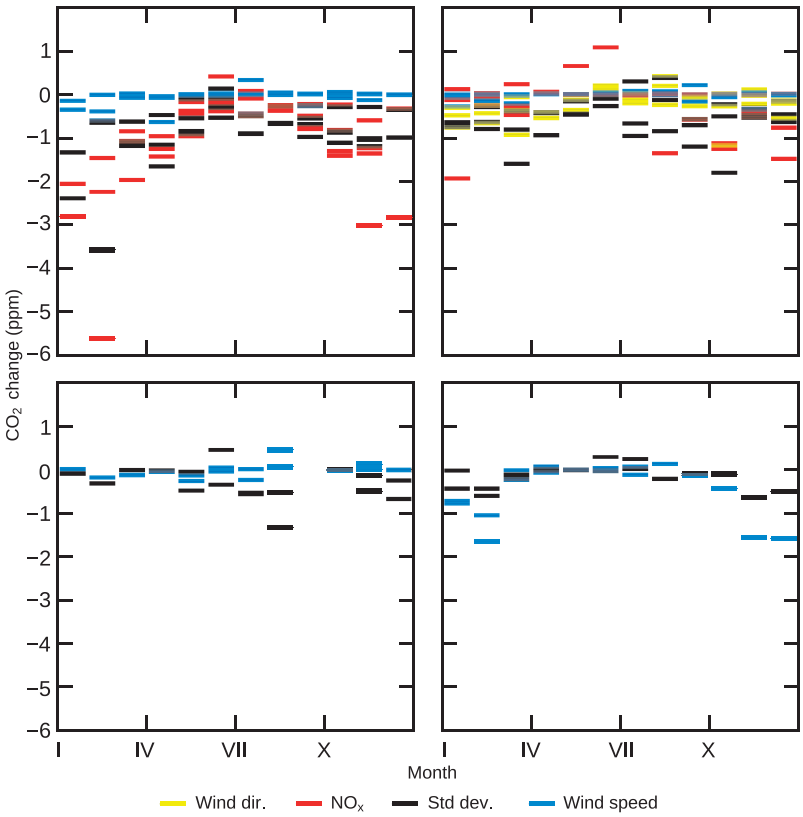

Fig. 5. The effects of CO_2 standard deviation, NO_x, wind speed, and wind direction filters, individually, on monthly averages over the whole measurement period.

filtered data. To summarize, the algorithm to estimate large-scale signals and seasonal variation was as follows:

1. Reject visually bad periods.
2. Select one-minute averages corresponding to suitable wind conditions (10-minute wind speed and direction).
3. Further select one-minute averages corresponding to low-pollution levels (Puijo and Kumpula).
4. Calculate the hourly means and standard deviation of selected values.
5. Select one-hour averages corresponding to low standard deviation.
6. Select afternoon hourly means with a difference of less than 3 standard deviations from the polynomial-harmonic function.
7. Calculate the daily means of the selected afternoon values (with the requirement of at least 3 hourly averages).
8. Select daily means with a difference of less than 3 standard deviations from the polynomial-harmonic function.
9. Calculate monthly means (at least 5 daily values).

Altogether, the filters flagged between 56% and 69% of hourly averages (Table 5). Individual filters changed monthly means from –6 ppm to 1 ppm (Fig. 5), negative changes in winter being the most systematic, particularly in Kumpula (Fig. 5a). The magnitude of these changes was significant in terms of contributing to individual source/sink estimations.

While selecting air samples based on meteorological variables can help to improve representativeness of the measurements, applying a constant threshold value is somewhat arbitrary. The uncertainty introduced by this method can be estimated by observing the variation of monthly mean values when the filters are modified: when aggressiveness of each filter is increased, wintertime averages increase and summertime values tend to decrease. The co-variation of filter parameters and CO_2 mole fraction

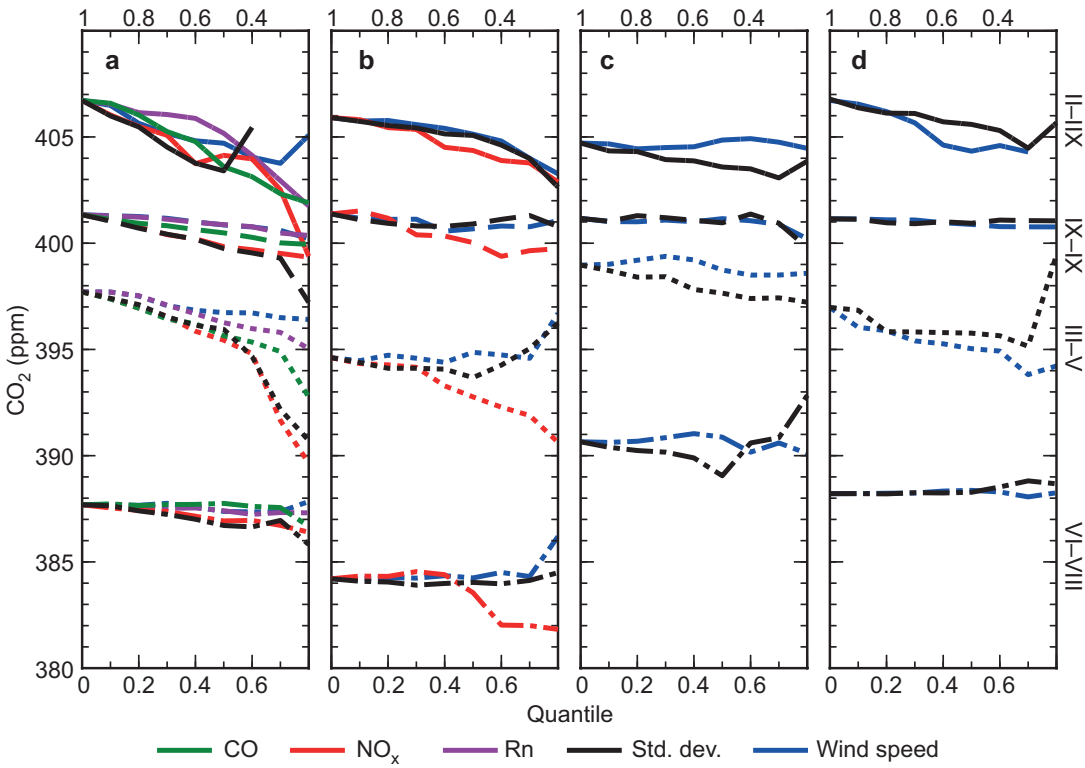

Fig. 6. The effects on monthly averages caused by CO_2 standard deviation, wind speed, NO_2, CO, and Rn filters, individually, increasing (CO, NO_2, Rn, std. dev.) or decreasing (wind speed) each filter parameter threshold by deciles, for winter (Dec–Feb, solid), spring (Mar–May, dotted), summer (June–Aug, dash-dotted), and autumn (Sep–Nov, dashed).

was examined by calculating monthly averages for each threshold decile.

Quantiles were determined for all four seasons separately, winter being defined as December, January and February. In Kumpula, the average mole fractions increased uniformly when any filter was gradually built up decile by decile (Fig. 6), suggesting that there is no self-evident choice for a threshold value. A relaxed filter was used here in order to retain enough data points to examine the seasonal variation of the polluted time series.

Seasonal variation

There was a distinct seasonal cycle at all the sites: the filtered monthly-average CO_2 mole fractions reached their maximums in midwinter and minimums in late summer (Fig. 7). The month-to-month variation was highest in the winter months, opposite to spring and summer. The biospheric uptake/respiration cycle of carbon is strongest in summer, masking larger-scale features. After the afternoon selection, together with wind speed and hourly standard deviation filters, the time series effectively followed the lower envelope of the summertime mole fractions at all continental sites. In winter, the variation from week to week was more apparent. Overall, monthly averages were similar to those in Pallas.

As compared with those at Pallas and other sites, the CO_2 mole fractions in Kumpula were much (2–3 ppm) higher in winter, and in summer they were 2–5 ppm higher than those in Puijo which is a similar site considering vegetation, although much higher above the surrounding terrain. We hypothesize that this difference was augmented by local anthropogenic sources. As compared with those at Pallas, using the filters specified in Table 5, the wintertime (December–

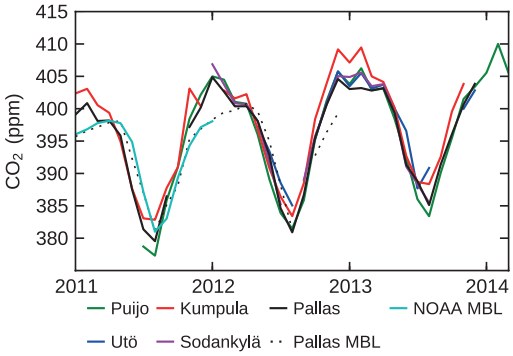

Fig. 7. Monthly-average CO_2 mole fractions. Pallas MBL (black, dotted line) is the Pallas time series with a marine air mass history as determined by trajectory analysis. NOAA MBL is shown at the latitude of Pallas.

February) mole fractions (weekly averages) at Kumpula were significantly higher (one-tailed *t*-test: $t_{19} = 4.1$, $p < 0.0001$). However, the wintertime averages of the sites converged when a more restrictive filtering was used (Fig. 6).

The lowest monthly-mean CO_2 mole fractions were found at Puijo in August 2011 and 2012 (0–2 ppm lower than the corresponding Pallas monthly means). This may be due to a relatively southern location with effective photosynthetic production and distance from the sea. While in winter, particularly filtering by air pollution (NO_x) systematically lowered the monthly-mean values at Puijo, the wind direction and NO_x filters had little effect in summer.

The summertime depression at the marine site Utö appeared shallower as compared with that at Pallas. The amplitude of the annual cycle was also the smallest, which can be attributed to a weaker summertime biogenic CO_2 depression, but the consistency of this difference cannot be assessed yet.

When Sammaltunturi measurements were selected for marine air mass history using atmospheric transport models, the seasonal cycle resembled the NOAA MBL. The greatest difference between filtered and MBL time series was in early-to-mid winter, when continental measurements were 4–6 ppm higher, presumably due to the wintertime sink in the northern Atlantic along with continuing respiration and attenuated photosynthesis in the NH continental source areas. In addition, the annual maxima in the MBL time series were reached later, in April–May. The general pattern was that the MBL time series (Pallas and NOAA) reached their summertime minima later as compared with the continental sites.

Summary and conclusions

The CO_2 mole fraction time series from four Finnish sites were examined for local and large-scale features. Of the four sites, Puijo and Sodankylä are within the boreal climate zone, Kumpula is a semi-urban site in the temperate broadleaf- and mixed-forest zone, and Utö is a marine site in the Baltic Sea. One to three years of data were available from all the sites, making seasonal comparisons possible.

To capture the features representing large-scale variations, the time series obtained from each site were masked using meteorological variables and air composition data to filter out local influences. Nighttime mole fractions, particularly at low tropospheric continental sites, reflect the fluxes from a very limited region. For this reason, only afternoon (12:00–18:00) mole fractions were considered.

We found that a CO_2 signal representing large-scale features can be extracted from most sites examined in this study, when filtered, masking periods that were associated with heavy influence by local fluxes. In particular, the time series obtained at the marine site Utö showed an indication of a robust large-scale signal. The selection routines suggested here can be used not only in finding large-scale features but also in regional studies. With the current regional network, it is potentially feasible to significantly reduce uncertainties and obtain realistic variability for inversed flux patterns over the Finnish boreal zone. In this work, high-frequency signals proved to be useful, or even necessary, in solving the regional-scale flux variability. Different steps of data selection from plain measurement error removal to extracting large-scale signals presented here may become useful, and ultimately it is the inverse modeling which can justify the involvement of different stations and their data selections in reducing the regional flux uncertainties. Overall, the current observations

represent a promising addition to data networks and deserve to be tested in atmospheric inversion modeling with an attempt to reduce regional flux uncertainties.

The Kumpula site, which is on the main building of the FMI, was an outlier, showing the strongest anthropogenic CO_2 signal. This was seen as high overall mole fractions, steep dependence of the mole fraction on air composition (NO_x, CO), large amplitude of the diurnal and seasonal cycles of the mole fraction, and larger median standard deviation of the hourly mole fraction, as compared with those at all the other sites in this study. Particularly wintertime mole fractions were high, and the *t*-test showed significant difference to correspondingly filtered Pallas time series, suggesting that the filtering scheme was not sufficient in masking local influences.

Where air pollution data were available (Puijo and Kumpula), the additional information on the air composition provided an opportunity to ignore air samples possibly associated with anthropogenic sources, particularly traffic. Although we only filtered with NO_x, utilizing simultaneous measurements of CO by modern gas analyzers may be feasible.

Acknowledgements: Authors would like to acknowledge Lauri Laakso, Timo Mäkelä, Juuso Rainne, ICOS 271878, ICOS-Finland 281255 and ICOS-ERIC 281250 funded by Academy of Finland and Finnish 719 Academy Center of Excellence (project no. 111865).

References

Aalto T., Hatakka J., Paatero I., Tuovinen J.-P., Aurela M., Laurila T., Holmén K., Trivett N. & Viisanen Y. 2002. Tropospheric carbon dioxide concentrations at a northern boreal site in Finland: basic variations and source areas. *Tellus* 54B: 110–126.

Aalto T., Lallo M., Hatakka J. & Laurila T. 2009. Atmospheric hydrogen variations and traffic emissions at an urban site in Finland. *Atmos. Chem. Phys.* 9: 7387–7396.

Ballantyne A.P., Alden C.B., Miller J.B., Tans P.P. & White J.W.C. 2012. Increase in observed net carbon dioxide uptake by land and oceans during the past 50 years. *Nature* 488: 70–72.

Beer C., Reichstein M., Tomelleri E., Ciais P., Jung M., Carvalhais N., Rodenbeck C., Arain M.A., Baldocchi D., Bonan G.B., Bondeau A., Cescatti A., Lasslop G., Lindroth A., Lomas M., Luyssaert S., Margolis H., Oleson K.W., Roupsard O., Veenendaal E., Viovy N., Williams C., Woodward F.I. & Papale D. 2010. Terrestrial gross carbon dioxide uptake: global distribution and covariation with climate. *Science* 329: 834–838.

Carouge C., Bousquet P., Peylin P., Rayner P.J. & Ciais P. 2010. What can we learn from European continuous atmospheric CO_2 measurements to quantify regional fluxes — Part 1: Potential of the 2001 network. *Atmos. Chem. Phys.* 10: 3107–3117.

Conway T.J., Tans P.P., Waterman L.S., Thoning K.W., Kitzis D.R., Masarie K.A. & Zhang N. 1994. Evidence for interannual variability of the carbon cycle from the National Oceanic and Atmospheric Administration/Climate Monitoring and Diagnostics Laboratory Global Air Sampling Network. *J. Geophys. Res.* 99: 22831–22855.

Crosson E.R. 2008. A cavity ring-down analyzer for measuring atmospheric levels of methane, carbon dioxide & water vapor. *Appl. Phys. B* 92: 403–408.

Eneroth K., Aalto T., Hatakka J., Holmén K., Laurila T. & Viisanen Y. 2005. Atmospheric transport of carbon dioxide to a baseline monitoring station in northern Finland. *Tellus* 57B: 366–374.

Haszpra L. 1999. On the representativeness of carbon dioxide measurements. *J. Geophys. Res.* 104: 26953–26960.

Hatakka J., Aalto T., Aaltonen V., Arain M., Hakola H., Komppula M., Laurila T., Lihavainen H., Paatero J., Salminen K. & Viisanen Y. 2003. Overview of the atmospheric research activities and results at Pallas GAW station. *Boreal Env. Res.* 8: 365–384.

Jung M., Reichstein M., Margolis H.A., Cescatti A., Richardson A.D., Arain M.A., Arneth A., Bernhofer C., Bonal D., Chen J., Gianelle D., Gobron N., Kiely G., Kutsch W., Lasslop G., Law B.E., Lindroth A., Merbold L., Montagnani L., Moors E.J., Papale D., Sottocornola M., Vaccari F. & Williams C. 2011. Global patterns of land atmosphere fluxes of carbon dioxide, latent heat & sensible heat derived from eddy covariance, satellite & meteorological observations. *J. Geophys. Res.* 116, doi: 10.1029/2010JG001566.

Keeling C.D., Bacastow R.B, Bainbridge A.E., Ekdahl C.A., Guenther P.R., Waterman L.S. & Chin J.F.S. 1976. Atmospheric carbon dioxide variations at Mauna Loa observatory, Hawaii. *Tellus* 28: 538–551.

Leskinen A., Portin H., Komppula M., Miettinen P., Arola A., Lihavainen H., Hatakka J., Laaksonen A. & Lehtinen K.E.J. 2009. Overview of the research activities and results at Puijo semi-urban measurement station. *Boreal. Env. Res.* 14: 576–590.

Luyssaert S., Inglima I., Jung M., Richardson A.D., Reichstein M., Papale D., Piao S.L., Schulze E.-D., Wingate L., Matteucci G., Aragao L., Aubinet M., Beer C., Bernhofer C., Black K.G., Bonal D., Bonnefond J.-M., Chambers J., Ciais P., Cook B., Davis K.J., Dolman A.J., Gielen B., Goulden M., Grace J., Granier A., Grelle A., Griffis T., Gruenwald T., Guidolotti G., Hanson P.J., Harding R., Hollinger D.Y., Hutyra L.R., Kolari P., Kruijt B., Kutsch W., Lagergren F., Laurila T., Law B.E., Le Maire G., Lindroth A., Loustau D., Malhi Y., Mateus J., Migliavacca M., Misson L., Montagnani L., Moncrieff J., Moors E., Munger J.W., Nikinmaa E., Ollinger

S.V., Pita G., Rebmann C., Roupsard O., Saigusa N., Sanz M.J., Seufert G., Sierra C., Smith M.-L., Tang J., Valentini R., Vesala T. & Janssens I.A. 2007. CO_2 balance of boreal, temperate & tropical forests derived from a global database. *Glob. Change Biol.* 13: 2509–2537.

Masarie K.A. & Tans P.P. Extension and integration of atmospheric carbon dioxide data into a globally consistent measurement record. 1995. *J. Geophys. Res.* 100: 11593–11610.

Masarie K.A., Pétron G. Andrews A., Bruhwiler L., Conway T. J., Jacobson A.R., Miller J.B., Tans P.P., Worthy D.E. & Peters W. 2011. Impact of CO_2 measurement bias on CarbonTracker surface flux estimates. *J. Geophys. Res.* 116, doi:10.1029/2011JD016270.

Paatero J., Hatakka J., Mattsson R. & Lehtinen I. 1994. A comprehensive station for monitoring atmospheric radioactivity. *Radiat. Protect. Dosim.* 54: 33–39.

Padin X.A., Vázquez-Rodríguez M., Ríos A.F. & Pérez F.F. 2007. Atmospheric CO_2 measurements and error analysis on seasonal air-sea CO_2 fluxes in the Bay of Biscay. *J. Marine Syst.* 66: 285–296.

Rella C.W., Chen H. Andrews A.E., Filges A., Gerbig C., Hatakka J., Karion A., Miles N.L., Richardson S.J., Steinbacher M., Sweeney C., Wastine B. & Zellweger C. 2013. High accuracy measurements of dry mole fractions of carbon dioxide and methane in humid air. *Atmos. Meas. Tech.* 6: 837–860.

Rödenbeck C., Houweling S., Gloor M. & Heimann M. 2003. CO_2 flux history 1982–2001 inferred from atmospheric data using a global inversion of atmospheric transport. *Atmos. Chem. Phys.* 3: 1919–1964.

Rödenbeck C., Conway T.J. & Langenfelds R.L. 2006. The effect of systematic measurement errors on atmospheric CO_2 inversions: a quantitative assessment. *Atmos. Chem. Phys.* 6: 149–161.

Thoning K.W., Tans P.P. & Komhyr W.D. 1989. Atmospheric carbon dioxide at Mauna Loa Observatory: 2. analysis of the NOAA GMCC data, 1974–1985. *J. Geophys. Res.* 94: 8549–8565.

Wesslander K. 2011. *The carbon dioxide system in the Baltic Sea surface waters*. Ph.D. thesis, Department of Earth Sciences, University of Gothenburg.